Review of Scientific Instruments

Electrostatic deflector studies using small-scale prototype electrodes

Cite as: Rev. Sci. Instrum. **90**, 045124 (2019); https://doi.org/10.1063/1.5086862
Submitted: 24 December 2018 . Accepted: 05 April 2019 . Published Online: 24 April 2019

K. Grigoryev, F. Rathmann, A. Stahl, and H. Ströher

Review of Scientific Instruments ARTICLE scitation.org/journal/rsi

Electrostatic deflector studies using small-scale prototype electrodes

Cite as: Rev. Sci. Instrum. 90, 045124 (2019); doi: 10.1063/1.5086862
Submitted: 24 December 2018 • Accepted: 5 April 2019 •
Published Online: 24 April 2019

K. Grigoryev,[1,a)] F. Rathmann,[1] A. Stahl,[2] and H. Ströher[1]

AFFILIATIONS

[1]Institute for Nuclear Physics, Forschungszentrum Jülich, 52425 Jülich, Germany
[2]III Physics Institute B, RWTH Aachen University, 52074 Aachen, Germany

[a)]**Electronic mail:** k.grigoryev@fz-juelich.de

ABSTRACT

The search for electric dipole moments of particles in storage rings requires the development of dedicated electrostatic deflector elements. The JEDI prototype-ring design consists of more than 50 electric deflectors of 1 m length with 60 mm spacing between the plates with electric fields of 10 MV m^{-1}. This paper presents studies of scaled-down uncoated prototype electrodes with 10 mm radius made of stainless steel. The electric field at electrode gap distances from 1 mm to 0.05 mm increased from 15 to 90 MV m^{-1}. In future investigations, we will study different materials and coatings at similar electrode spacings. Preparations are also underway to study large deflector elements.

I. INTRODUCTION

The JEDI collaboration[1] is searching for permanent electric dipole moments (EDMs) of charged particles, such as protons[2] and deuterons.[3] One of the technical challenges is the development of electric bending elements that provide high electric fields. A purely electrostatic EDM ring of 30 m radius, for instance, requires electric fields of about 17 MV m^{-1}.[4] The present limit for the electric field of bending elements at accelerators is below 10 MV m^{-1}.[5] The electrostatic separators at CESR[6,7] and Fermilab[8] Tevatron,[9,10] and the CERN septa[11] are routinely operated at smaller electric fields.

In order to study different electrode materials and coatings, the investigations described here made use of scaled-down prototypes and a dedicated UHV test stand installed inside a clean room at RWTH Aachen University. The operation in the laboratory with respect to radiation protection was simplified because the applied voltages were always below 30 kV. Nevertheless, by scaling down the applied voltage and by reducing at the same time the spacing between the electrodes, large electric fields could be obtained.

In Sec. II, the experimental setup is described. General considerations of the deflector development are given in Sec. II A. The electrical scheme using a high-voltage power supply is discussed in Sec. II B, and the setup of the vacuum system inside a clean room is described in Sec. II C. The electrodes are presented in Sec. III, and the measurements are presented in Sec. IV. The results are summarized in Sec. V.

II. EXPERIMENTAL SETUP

A. Small-scale prototype electrodes

Initial investigations about the shape of electrostatic deflectors were based on existing elements used at the Fermilab Tevatron.[12] The plates of the Tevatron electrostatic separators were designed to provide a field of 6 MV m^{-1} at distances of 40–60 mm with a length of about 2.5 m. The transverse profile of the Tevatron separators represents a Rogowski profile.[13] For a specific electrode configuration (i.e., plate separation and height), the surface contour of the electrodes is designed to follow the equipotential lines. Such a profile ensures a high homogeneity of the electric field in the flat region between the deflector plates, and, according to Refs. 14 and 15, a discharge will occur *outside* of that region.

In order to simplify the mechanical production of prototype elements for the test setup at RWTH Aachen University, all elements were manufactured with round corners rather than with Rogowski profiles. The smallest elements consist of half-spheres with a radius of $R = 10$ mm. Small test samples also served to minimize weight which eliminated the need for a sophisticated support structure.

B. Electrical scheme

Numerical simulations of the electric field E, performed with the QuickField FEA software,[16] showed that for our studies, there

is essentially no difference between using the same but opposite potentials U_0 between the electrodes or having one of the electrodes powered with twice the voltage $2U_0$, while the other one is grounded (see Fig. 1).

The option with one grounded electrode [see Fig. 1(b)] is more attractive because the measurements can then be performed with a single high-voltage power supply. In addition, common ground for every device minimizes the measurement noise and makes the dark current detection with a picoammeter[17] more reliable.

The electrical circuit, shown in Fig. 2, consists of two discharge protection elements. The 100 MΩ resistor serves to limit the current to ground during high voltage (HV) breakdown. The gas discharge boxes[18] and the low-leakage diodes[19] protect the picoammeter from high currents during a discharge.

To ensure safe operation, the high-precision high-voltage power supply[20] was equipped with a rapid discharge circuit. A fast discharging capacitor within the power supply reduces the voltage to less than 1% of the applied value in less than 1 s. The measured voltage ripple of the power supply was below the specified value of 10^{-4} at 30 kV and was stabilized to better than 0.05% over a time interval of 8 h.

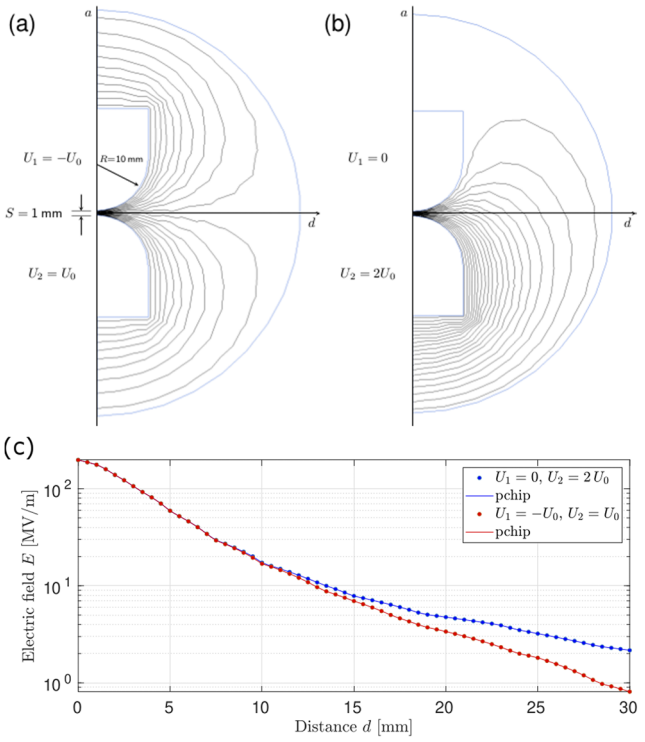

FIG. 1. Equipotential lines using QuickField[16] for the different potential configurations with R = 10 mm, S = 1 mm, and U_0 = 10 kV. The electrodes are rotationally symmetric around the axis a. Panel (a): the electrodes at the same but opposite potentials U_0. Panel (b): one of the electrodes is grounded and another powered with twice the voltage U_0. The electric field E as a function of distance d for both cases shown in panels (a) and (b) with a piecewise cubic hermite interpolating polynomial (pchip) is depicted in panel (c).

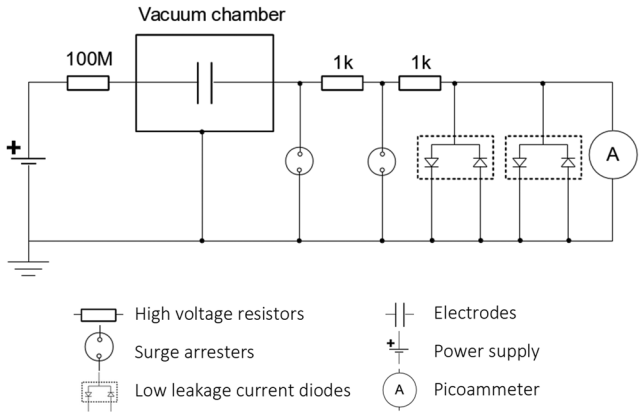

FIG. 2. Electrical schematic of the test apparatus used for the measurements. A 100 MΩ resistor, two gas discharge boxes acting as surge arresters[18], and two low-leakage diodes[19] are used to protect the power supply and the picoammeter during voltage breakdown in an electric discharge.

C. Clean room and vacuum system

To perform the test measurements, a 25 m^2 class ISO7[21] clean room was installed in the experimental hall at RWTH Aachen University with a gateway and a strip curtain for rolling the test apparatus (see Fig. 3). The clean area inside was sufficiently large to place a few tables besides the test stand for the prototypes.

A dust-free vacuum system was designed and built using UHV components, mounted on a movable support for easy access and flexibility during the measurements [see Fig. 4(a)]. An oil-free turbomolecular pump[22] with 300 ℓ/s pumping speed and air cooling, backed by a dry scroll pump[23] with 15 $m^3\ h^{-1}$ pumping speed, allowed us to reach good vacuum conditions within a few minutes. Simultaneous heating of the chamber to the maximum operating temperature of the turbopump (80 °C) removed water from the stainless-steel walls of the vacuum chamber and brought the pressure down to about 10^{-9} mbar.

A 300 ℓ/s ion-getter pump,[24] installed directly on the vacuum chamber, was activated at the same time when the vacuum chamber

FIG. 3. Class ISO7[21] clean room at RWTH Aachen University, housing the experimental setup for electrostatic tests.

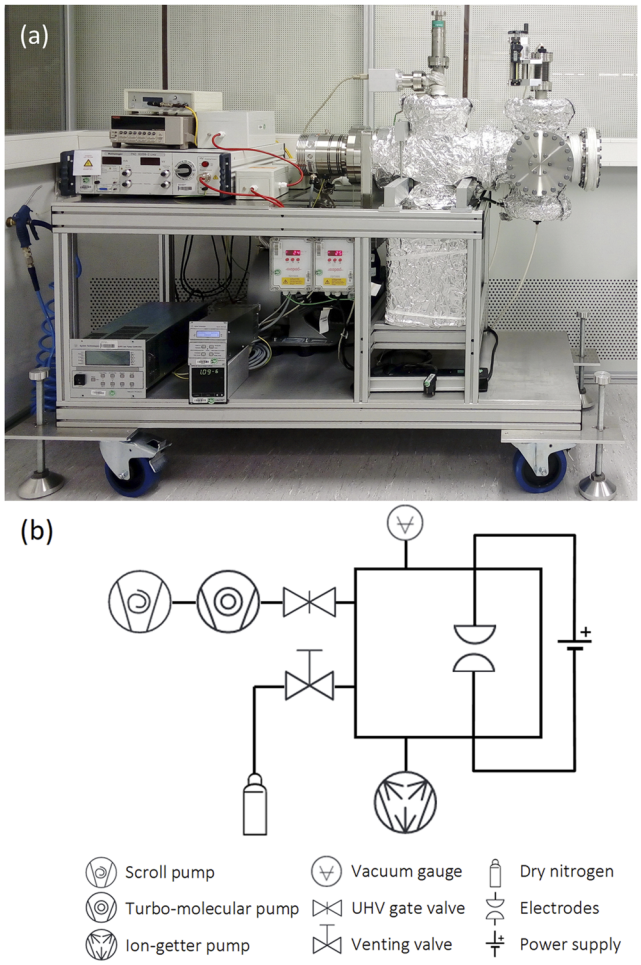

FIG. 4. Experimental test bench in the clean room to study small scale prototype electrodes at RWTH Aachen University. (a) Photograph of the experimental test bench. (b) Schematic of the vacuum system.

was baked out. After activation of the ion-getter pump, the vacuum chamber was isolated from the scroll and turbomolecular pumps using a UHV gate-valve[25] [see Fig. 4(b)], and the pressure reached about 10^{-11} mbar. During the tests, the scroll and turbomolecular pumps were turned off to minimize vibrations. The pressure in the vacuum chamber, measured directly by the ion-getter pump, was typically of the order of 10^{-10} mbar.

III. TEST ELECTRODES

The electrodes for the tests were made of stainless steel in two different sizes. The small ones are half-spheres of radius $R = 10$ mm. The large electrodes additionally possess a flat central region of 20 mm diameter. Based on the experience reported in Refs. 26 and 27, for further investigations, a set of stainless-steel samples prepared in the same way was coated with TiN (see Fig. 5). The results of the measurements using stainless steel and

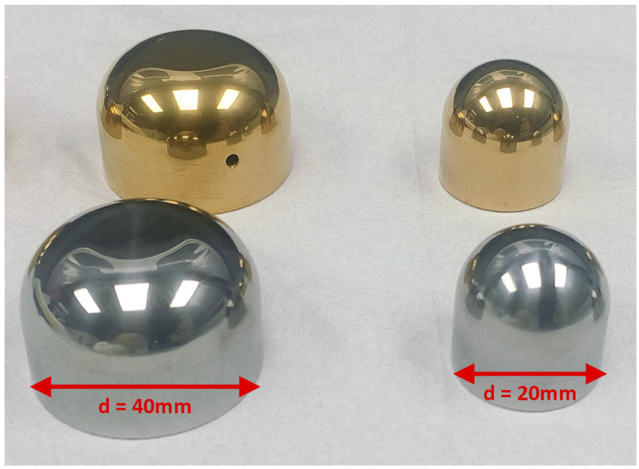

FIG. 5. Stainless-steel electrode prototypes. The uncoated elements are shown in the front, and the TiN coated elements are shown in the back.

aluminum coated with TiN will be described in a forthcoming publication.

The test electrodes were produced and mechanically polished in the RWTH Aachen workshop. The average roughness of the surface was smaller than 0.10 μm with a maximum nonuniformity of 1.17 μm. Prior to installation into the vacuum chamber, all parts were cleaned in an ultrasonic propanol bath.

For precise positioning, each measurement started by mechanically setting the distance between the electrodes to zero. This was accomplished by applying a small voltage and observation of a large current at the picoammeter when the electrodes touched each other. From there, one of the electrodes was moved to the measurement position using a manual UHV-compatible linear drive[28] with 0.01 mm positioning accuracy.

The electric field between the two half-spherical electrodes can be written as[29]

$$E_{\max} = \frac{U}{S} \cdot F, \tag{1}$$

where F denotes the so-called field enhancement factor, U is the voltage, and S is the spacing between the electrodes. The field enhancement factor F can be calculated for known shapes. For half-spherical electrodes with radius of curvature R,[30]

$$F = \frac{1}{4}\left[1 + \frac{S}{R} + \sqrt{\left(1 + \frac{S}{R}\right)^2 + 8}\right], \tag{2}$$

where S denotes the spacing between the two spheres, so that the distance between the centers of the half-spheres is given by

$$D = S + 2R. \tag{3}$$

At the employed distances between 0.1 and 1 mm, the field enhancement factor F changes only by about 3% (see Fig. 6).

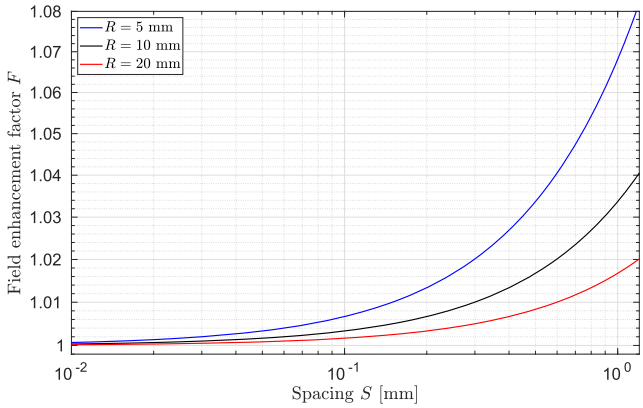

FIG. 6. Field enhancement factor F as a function of spacing S between two ideal half-spheres of radii R = 5, 10, and 20 mm.

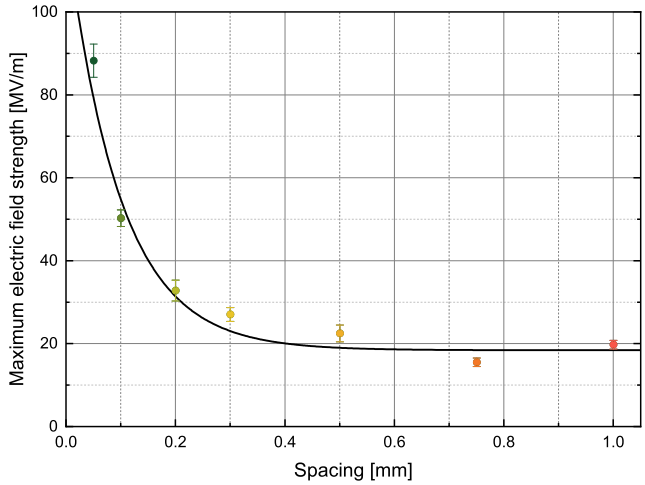

FIG. 8. Maximum electric field strength from Fig. 7 as a function of spacing between the half-sphere stainless-steel electrodes of R = 10 mm radius. The values of E_{max} computed using Eq. (1) and F from Eq. (2) correspond to zero dark current. For the individual points, the same colors as in Fig. 7 were taken. The line is drawn to guide the eye.

IV. DARK CURRENT MEASUREMENTS

For the measurements, the experimental setup was transferred to the COSY hall at Forschungszentrum Jülich. The first high-voltage tests were performed with well-polished stainless-steel half-sphere electrodes over a wide range of distances ranging from S = 30 mm to 0.05 mm (see Fig. 7). Being limited by the 30 kV power supply, the discharges mainly happened in the test conditions with small gaps between the electrodes. No discharge was observed at a distance S = 10 mm with an applied voltage of 30 kV which leads to $E_{max} \approx 4.1$ MV m^{-1}. Discharges at larger distances can only be observed when higher voltages are applied which requires a new experimental setup.

For completeness, tests were also carried out by replacing one of the half-sphere electrodes with the larger stainless-steel electrodes with a flat surface (see Fig. 5). In that case, the measured electric field behaved in a similar way and reached values which likely correspond to vacuum breakdown conditions.[31,32]

The measured minimal dark currents were compatible with zero to tenths of a picoampere (see Fig. 7). The maximum values of the electric field E_{max}, shown in Fig. 8 and calculated using Eq. (1) and F from Eq. (2), are taken at the measurement points when the dark current was still compatible with zero within errors. The measurements showed that with half-sphere electrodes of 10 mm radius at distances of less than a millimeter, electric fields above the required values of E = 17 MV m^{-1} could be reached.

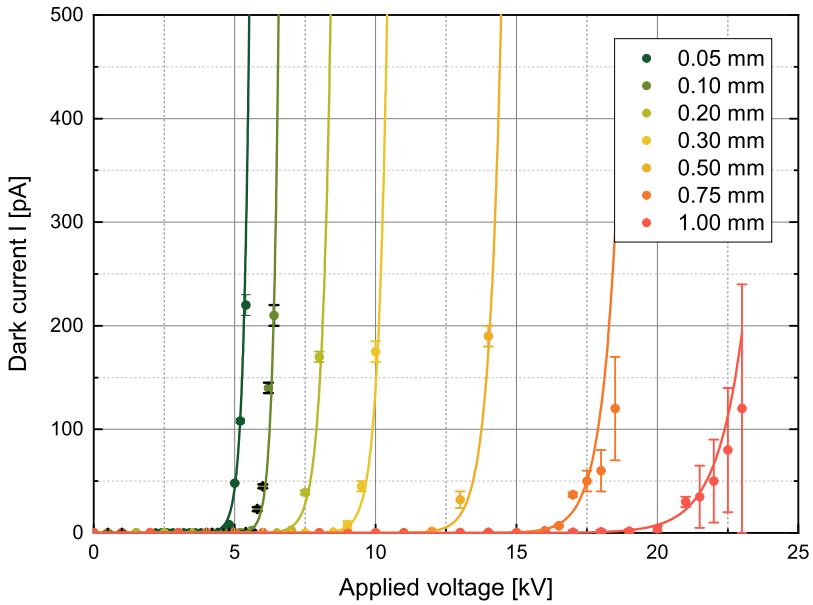

FIG. 7. Dark current measured using stainless-steel half-sphere electrodes of R = 10 mm radius at distances S = 0.05–1 mm.

The maximum electric fields obtained at a distance S = 0.05 mm, however, are still an order of magnitude smaller than achieved elsewhere[33] at much smaller distances of S = 0.02 mm. It should be noticed that with respect to the development of electrostatic deflector elements for the future EDM ring, the region of interest ranges from a few centimeter to about 10 cm distance, which can be studied only with large deflectors and much higher applied voltages.

V. SUMMARY

Mechanically polished stainless-steel electrodes at distances less than a millimeter demonstrate that electric fields close to the breakdown limit in ultrahigh vacuum can be reached. The maximum electric fields obtained in the measurements using scaled-down electrodes look promising. They are clearly above the required values for an electrostatic deflector of 17 MV m^{-1} for a future EDM ring of 30 m radius. The improvement of the HV breakdown capability using different electrode materials and coatings as well as gas conditioning will be further investigated in the future.

We will now move on to measurements with real-size deflector elements of a length ℓ = 1020 mm at distances of $S \approx$ 20–120 mm between the plates. A suitable experimental infrastructure with two 200 kV power supplies is presently setup at IKP of Forschungszentrum Jülich.

ACKNOWLEDGMENTS

This work has been performed in the framework of the JEDI collaboration and is financially supported by an ERC Advanced-Grant (srEDM No. 694390) of the European Union.

REFERENCES

[1] See http://collaborations.fz-juelich.de/ikp/jedi for Jülich Electric Dipole moment Investigations.
[2] V. Anastassopoulos, S. Andrianov, R. Baartman, S. Baessler, M. Bai, J. Benante, M. Berz, M. Blaskiewicz, T. Bowcock, K. Brown, B. Casey, M. Conte, J. D. Crnkovic, N. D'Imperio, G. Fanourakis, A. Fedotov, P. Fierlinger, W. Fischer, M. O. Gaisser, Y. Giomataris, M. Grosse-Perdekamp, G. Guidoboni, S. Hacıömeroğlu, G. Hoffstaetter, H. Huang, M. Incagli, A. Ivanov, D. Kawall, Y. I. Kim, B. King, I. A. Koop, D. M. Lazarus, V. Lebedev, M. J. Lee, S. Lee, Y. H. Lee, A. Lehrach, P. Lenisa, P. L. Sandri, A. U. Luccio, A. Lyapin, W. MacKay, R. Maier, K. Makino, N. Malitsky, W. J. Marciano, W. Meng, F. Meot, E. M. Metodiev, L. Miceli, D. Moricciani, W. M. Morse, S. Nagaitsev, S. K. Nayak, Y. F. Orlov, C. S. Ozben, S. T. Park, A. Pesce, E. Petrakou, P. Pile, B. Podobedov, V. Polychronakos, J. Pretz, V. Ptitsyn, E. Ramberg, D. Raparia, F. Rathmann, S. Rescia, T. Roser, H. K. Sayed, Y. K. Semertzidis, Y. Senichev, A. Sidorin, A. Silenko, N. Simos, A. Stahl, E. J. Stephenson, H. Ströher, M. J. Syphers, J. Talman, R. M. Talman, V. Tishchenko, C. Touramanis, N. Tsoupas, G. Venanzoni, K. Vetter, S. Vlassis, E. Won, G. Zavattini, A. Zelenski, and K. Zioutas, Rev. Sci. Instrum. **87**(11), 115116 (2016).
[3] F. Rathmann and N. Nikolaev, "Precursor experiments to search for permanent electric dipole moments (EDMs) of protons and deuterons at COSY," in 8th International Conference on Nuclear Physics at Storage Rings (STORI11), PoS STORI11 (2011) 029, 2011.
[4] F. Rathmann, A. Saleev, and N. N. Nikolaev, Phys. Part. Nucl. **45**, 229 (2014).
[5] M. Reiser, *Theory and Design of Charged Particle Beams*, 2nd ed. (Wiley Series in Beam Physics and Accelerator Technology, Wiley, 2008).
[6] See https://www.classe.cornell.edu/public/lab-info/cesr.html for Cornell Electron-positron Storage Ring.
[7] J. J. Welch, G. W. Codner, and W. Lou, "Commissioning and performance of low impedance electrostatic separators for high luminosity at CESR," in 1999 Particle Accelerator Conference (PAC'99), New York, March 29–April 2, 1999.
[8] See http://www.fnal.gov for Fermi National Accelerator Laboratory.
[9] V. Lebedev and V. Shiltsev, *Accelerator Physics at the Tevatron Collider, Particle Acceleration and Detection* (Springer, New York, 2014).
[10] V. Shiltsev, Y. Alexahin, V. Lebedev, P. Lebrun, R. S. Moore, T. Sen, A. Tollestrup, A. Valishev, and X. L. Zhang, Phys. Rev. Spec. Top.–Accel. Beams **8**, 101001 (2005), 266.
[11] J. Borburgh, M. Hourican, and A. Prost, "Final results on the CERN PS electrostatic septa consolidation program," in Particle Accelerator Conference, C030512, 2003.
[12] O. Prokofiev, Tevatron beam separator R&D; available from https://www.bnl.gov/edm/review/files/references/Prokofiev_separator_R&D_dec6_2005.pdf, 2005.
[13] N. G. Trinh, IEEE Trans. Power Appar. Syst. **PAS-99**(3), 1235 (1980).
[14] W. Rogowski, Arch. Elektrotech. **12**(1), 1 (1923).
[15] W. Rogowski, Arch. Elektrotech. **16**(1), 73 (1926).
[16] See https://quickfield.com for QuickField simulation software, Tera Analysis Ltd.
[17] See https://www.tektronix.com for Keithley picoammeter 6485.
[18] See https://tdk-electronics.tdk.com for EPCOS AG, type EPCOS EC90X and EC600X.
[19] See https://www.diodes.com for Diodes Incorporated, type BAV199.
[20] See https://www.heinzinger.com/products/high-voltage/universal-high-voltage-power-supplies for Heinzinger PNC 30000.
[21] A class ISO7 clean room allows inside 1 m^3 of air, a maximum of 10^7 particles of size >0.1 μm, and not more than 352 000 particles of size >0.5 μm.
[22] See https://www.agilent.com for Agilent TwisTorr 304.
[23] See https://www.agilent.com for Agilent TriScroll 300.
[24] See https://www.agilent.com for Agilent Vaclon Plus 300.
[25] See https://www.vacom.de for Vacom 5GVM-160CF-MV-S, copper sealed ultra-high vacuum hand gate-valve.
[26] F. Furuta, T. Nakanishi, S. Okumi, T. Gotou, M. Yamamoto, M. Miyamoto, M. Kuwahara, N. Yamamoto, K. Naniwa, K. Yasui, H. Matsumoto, M. Yoshioka, and K. Togawa, Nucl. Instrum. Methods Phys. Res., Sect. A **538**(1), 33 (2005).
[27] M. A. A. Mamun, A. A. Elmustafa, R. Taus, E. Forman, and M. Poelker, J. Vac. Sci. Technol., A **33**(1), 031604 (2015).
[28] See http://www.uhvdesign.com for Compact linear drive CLSM38-50-H-DLA from UHV Design.
[29] A. Russell, J. Inst. Electr. Eng. **65**, 517 (1927).
[30] General Electric Company, *General Electric Review, 1913* (Forgotten Books, 2018), see https://www.amazon.com/dp/0365105678.
[31] G. R. Werner, "Probing and modeling voltage breakdown in vacuum," Ph.D. thesis, Cornell University Laboratory for Elementary-Particle Physics, 2004.
[32] J. Meek and J. Craggs, *Electrical Breakdown of Gases* (A Wiley-Interscience publication, Wiley, 1978).
[33] A. Descoeudres, T. Ramsvik, S. Calatroni, M. Taborelli, and W. Wuensch, Phys. Rev. Spec. Top.–Accel. Beams **12**, 032001 (2009), 148.